Food and Chemical Toxicology 164 (2022) 113017

Contents lists available at ScienceDirect

Food and Chemical Toxicology

journal homepage: www.elsevier.com/locate/foodchemtox

Kaempferol prevents the activation of complement C3 protein and the generation of reactive A1 astrocytes that mediate rat brain degeneration induced by 3-nitropropionic acid

Carmen Lopez-Sanchez [a,b,*,1], Joana Poejo [a,1], Virginio Garcia-Lopez [a,b], Jairo Salazar [a,c], Virginio Garcia-Martinez [a,b], Carlos Gutierrez-Merino [a,d,**]

[a] Instituto de Biomarcadores de Patologías Moleculares, Universidad de Extremadura, 06006, Badajoz, Spain
[b] Departamento de Anatomía y Embriología Humana, Facultad de Medicina, Universidad de Extremadura, 06006, Badajoz, Spain
[c] Departamento de Química, Universidad Nacional Autónoma de Nicaragua-León, León, 21000, Nicaragua
[d] Departamento de Bioquímica y Biología Molecular y Genética, Facultad de Ciencias, Universidad de Extremadura, 06006, Badajoz, Spain

ARTICLE INFO

Handling Editor: Dr. Jose Luis Domingo

Keywords:
Kaempferol
3-Nitropropionic acid
Wistar rats
C3 protein
Reactive A1 astrocytes
Amyloid β peptides

ABSTRACT

Kaempferol is a natural antioxidant present in vegetables and fruits used in human nutrition. In previous work, we showed that intraperitoneal (i.p.) kaempferol administration strongly protects against striatum neurodegeneration induced by i.p. injections of 3-nitropropionic acid (NPA), an animal model of Huntington's disease. Recently, we have shown that reactive A1 astrocytes generation is an early event in the neurodegeneration induced by NPA i.p. injections. In the present work, we have experimentally evaluated the hypothesis that kaempferol protects both against the activation of complement C3 protein and the generation of reactive A1 astrocytes in rat brain striatum and hippocampus. To this end, we have administered NPA and kaempferol i.p. injections to adult Wistar rats following the protocol described in previous work. Kaempferol administration prevents proteolytic activation of complement C3 protein and generation of reactive A1 astrocytes NPA-induced in the striatum and hippocampus. Also, it blocked the NPA-induced increase of NF-κB expression and enhanced secretion of cytokines IL-1α, TNFα, and C1q, which have been linked to the generation of reactive A1 astrocytes. In addition, kaempferol administration prevented the enhanced production of amyloid β peptides in the striatum and hippocampus, a novel finding in NPA-induced brain degeneration found in this work.

1. Introduction

Kaempferol is a natural antioxidant of the flavonoids group of flavonols that is present in many vegetables and fruits widely used in human nutrition. In previous work, we reported that intraperitoneal (i.p.) kaempferol administration strongly protects against brain neurodegeneration of the striatum induced by i.p. injections of 3-nitropropionic acid (NPA) [Lagoa et al., 2009]. Also, we have shown that intravenous administration of kaempferol affords a large attenuation of brain damage induced by ischemia-reperfusion in a rat model of transient focal ischemia caused by occlusion of the middle cerebral artery [Lopez-Sanchez et al., 2007]. Due to kaempferol's low toxicity in humans, we suggested that this compound bears a significant potential therapeutic use as a protective agent against brain damage induced by some insults and/or some neurodegenerative diseases. Indeed, therapeutic applications of kaempferol have been reviewed recently, with particular emphasis on its anti-inflammatory effects [Ren et al., 2019; Silva Dos Santos et al., 2021].

The compound NPA is a neurotoxin produced by some fungi and plants that can cause severe intoxication of cattle and humans [Ludolph et al., 1991; He et al., 1995]. The systemic administration of NPA to rodents and non-human primates produces neurological dysfunctions that closely mimic some neurological alterations found in human Huntington's disease (HD) [Brouillet et al., 1999, 2005]. Thus, systemic administration of NPA to rodents has been used as an animal model to study the molecular and cellular mechanisms underlying the brain neurodegeneration observed in this disease. Striatum degeneration is a

* Corresponding author. Instituto de Biomarcadores de Patologías Moleculares, Universidad de Extremadura, 06006, Badajoz, Spain.
** Corresponding author. Instituto de Biomarcadores de Patologías Moleculares, Universidad de Extremadura, 06006, Badajoz, Spain.
E-mail addresses: clopez@unex.es (C. Lopez-Sanchez), carlosgm@unex.es (C. Gutierrez-Merino).
[1] Both should be considered first authors.

https://doi.org/10.1016/j.fct.2022.113017
Received 14 December 2021; Received in revised form 7 April 2022; Accepted 11 April 2022
Available online 19 April 2022

Abbreviations

Aβ	Amyloid β peptide;
APP	Amyloid β Precursor Protein
ATP	Adenosine triphosphate
BSA	Bovine Serum Albumin
b.w.	bodyweight
C1q	Complement protein component 1q
C3	Complement protein component 3
COX-2	Cyclooxygenase-2
GFAP	Glial Fibrillary Acidic Protein
HD	Huntington's Disease
i.p.	Intraperitoneal
IL-1α	Interleukin 1 alpha
iNOS	inducible Nitric Oxide Synthase
NBT/BCIP	Nitroblue Tetrazolium/5-Bromo-4-Chloro-3-Indolyl Phosphate
NF-κB	Nuclear Factor kappa B
NOS	Nitric Oxide Synthase
NPA	3-Nitropropionic Acid
PBS	Phosphate-Buffered Saline;
PVDF	Polyvinylidene Difluoride;
ROS	Reactive Oxygen Species
SDS	Sodium Dodecyl Sulfate
SDS-PAGE	Sodium Dodecyl Sulfate-Polyacrylamide Gel Electrophoresis
SEM	standard error of the mean
TNFα	Tumor Necrosis Factor-alpha
TBS	Tris-buffered Saline;
TBST	TBS supplemented with 0.05% Triton X-100
TTC	2,3,5-Triphenyltetrazolium Chloride.

major common feature found in NPA-treated rats and HD [Brouillet et al., 2005]. Subsequently, it has been shown that systemic administration of NPA also elicits metabolic alterations in cortical areas adjacent to the striatum, as well as in the hippocampus and the cerebellum [Tsang et al., 2009; Menze et al., 2015]. This correlates with cognitive dysfunction, visuospatial deficits, memory loss, and difficulty in learning new skills, reported in pre-motor stages of HD [Ho et al., 2003; Phillips et al., 2008].

Neuroinflammation is a common cause of tissue stress in brain neurodegeneration that contributes to spreading an initially focalized neuronal insult widely, and it has been shown that NPA administration induces the activation of neuroinflammatory microglia [Ryu et al., 2003; Chakraborty et al., 2014; Jin et al., 2018], an activation which has also been reported in the striatum and vicinal cortical areas in HD patients [Niccolini and Politis, 2014]. Activated microglia secretes pro-inflammatory cytokines and enhances reactive oxygen species (ROS) and nitric oxide production in the brain [Liu et al., 2002], and oxidative stress caused by ROS overproduction has been shown to mediate NPA-induced brain neurodegeneration [Nasr et al., 2003; Rosenstock et al., 2004; Brouillet et al., 2005; Lagoa et al., 2009]. Furthermore, intracellular oxidative stress elicited by mitochondrial dysfunction is known to activate the nuclear factor kappa B (NF-κB) signaling pathway [Gutierrez-Merino et al., 2011], and NF-κB activation leads to enhanced secretion of the pro-inflammatory cytokines that mediate NPA-induced brain degeneration [Ryu et al., 2003; Chakraborty et al., 2014; Jin et al., 2018]. Indeed, i.p. administration of NPA-induced degeneration of the striatum in adult Wistar rats produces a high decline of reduced glutathione, as well as a noticeable elevation of protein nitrotyrosines [Lagoa et al., 2009]. Also, an excess of ROS and nitric oxide causes both reversible and irreversible damage to the mitochondrial respiratory chain function [Stewart et al., 2002], and this further potentiates NPA neurotoxicity, since NPA impairs the mitochondrial respiratory chain directly, acting as an irreversible inhibitor of succinate dehydrogenase [Brouillet et al., 2005]. In addition, the inhibition of creatine kinase activity accelerates the neuronal energetic crisis in this nitroxidative scenario leading to a sustained ATP depletion that induces rapid cell death [Lagoa et al., 2009]. Since many flavonoids are well-known inhibitors of proinflammatory cytokines, inducible nitric oxide synthase (iNOS), as well as cyclooxygenase-2 (COX-2) gene expression in the brain through inhibition of NF-κB activation, as reviewed in Gutierrez-Merino et al. (2011), it could be expected that flavonoids provide protection against brain neurodegeneration induced by systemic NPA-administration. Interestingly, when we administered i.p. kaempferol, it effectively protects against striatum degeneration and motor neurological dysfunctions induced by NPA administration, by preventing the decrease of reduced glutathione, the increase of protein nitrotyrosines, and the inhibition of creatine kinase activity [Lagoa et al., 2009]. We also reported that intravenous administration of kaempferol elicits a large inhibition of protein nitrotyrosines production in brain lesion areas during the insult of transient focal cerebral ischemia [Lopez-Sanchez et al., 2007]. In agreement, *Ginkgo biloba* extract EGb761, in which kaempferol is one of the most abundant flavonoids, presents neuroprotective properties in brain ischemia models [Saleem et al., 2008]. Although brain inflammation is found in many neurodegenerative diseases, the anti-inflammatory effects of flavonoids have been reported in many mammalian cell types and are not tissue-specific, reviewed in Maleki et al. (2009).

In the last few years, it has been shown that some neuroinflammatory cytokines secreted by activated microglia in the brain can induce the generation of reactive A1 astrocytes that are highly neurotoxic [Zhang et al., 2014; Bennett et al., 2016; Liddelow et al., 2017]. Liddelow et al. (2017) demonstrated that three cytokines secreted by activated microglia, interleukin-1α (IL-1α), tumor necrosis factor α (TNFα), and complement component 1q (C1q), acting together are necessary and sufficient to induce the generation of the highly neurotoxic reactive A1 astrocytes. This bears a special relevance for brain degeneration because astrocytes are the most abundant brain cells and are necessary for neuronal survival and functioning, and for the maintenance of the blood-brain barrier integrity [Hawkins and Davis 2005]. Indeed, astrocytes are increasingly viewed as critical contributors to neurological disorders [Escartin et al. 2021] and can secrete pro-inflammatory mediators that induce neuroinflammation and result in disruption in tight junctions, finally leading to blood-brain barrier integrity breakdown and brain edema formation [Farina et al. 2007; Lee and MacLean 2015]. Neurotoxic reactive A1 astrocytes are abundant in post-mortem tissue of HD patients and, also, of Alzheimer's disease [Liddelow et al., 2017]. Astrocytes dysfunctions or gliosis have been reported in the striatum of rats treated with systemic administration of NPA [Fu, 1995; Nishino et al., 1997; Lagoa et al., 2009; Jin et al., 2018; Lopez-Sanchez et al., 2020]. Recently, we have shown that the induction of reactive A1 astrocytes in the striatum, hippocampus, and cerebellum of rat brains by NPA i.p. precedes the brain damage leading to motor neurological dysfunctions in the NPA-induced neurodegeneration [Lopez-Sanchez et al., 2020]. Furthermore, it has been recently shown that reactive astrocytes induced by 2-chloroethanol poisoning can stimulate microglia polarization [Wang et al., 2021]. Thus, reactive astrocytes induced by chemical insults can also further potentiate the activation of microglia leading to a feed-forward cycle harmful to specific brain structures. However, the possibility that kaempferol administration could prevent the generation of reactive A1 astrocytes in NPA-induced brain neurodegeneration has not been experimentally assessed in previous works. In addition, reactive astrocytes can produce neurotoxic amyloid β peptides

[Nadler et al., 2008; Zhao et al., 2011; Frost and Li, 2017], and this possibility deserved to be studied in NPA-induced brain neurodegeneration because it has been shown recently that this neurodegenerative process is also a tauopathy [Lahiani-Cohen et al., 2020].

Complement C3 protein gene expression is highly upregulated in reactive A1 astrocytes [Liddelow et al., 2017]. Thus, C3 protein expression has been used as a specific marker of reactive A1 astrocytes generation, as reported in post-mortem tissue of HD patients, in which abundant reactive A1 astrocytes have been identified [Liddelow et al., 2017]. Nevertheless, it has to be recalled that complement C3 protein is initially produced in an inactive form that, to be activated, requires partial proteolysis [Huber-Lang et al., 2018]. In addition to the classical/lectin and alternative pathway C3 proteases that produce the larger C3α fragments (C4bC2a and C3bBb, respectively), other proteases have been shown to act as auxiliary proteases producing further cleavage of C3 [Huber-Lang et al., 2018]. Several of these proteases are activated and/or released into the extracellular medium during brain neurodegenerative processes, such as extracellular metalloproteases [Rosenberg, 2009] and cathepsins [Nakanishi, 2020]. To the best of our knowledge, the possibility that flavonoids can be potent inhibitors of the pathways (classical or alternative) of C3 activation has been overlooked to date, although some medicinal plants have been shown to contain active ingredients such as flavonoids, among others, which are inhibitors of the complement system activation [Kulkarni et al., 2005].

On these grounds, we hypothesized that kaempferol may protect against both the activation of complement C3 protein and the generation of reactive A1 astrocytes in the brain regions, striatum, hippocampus, that become dysfunctional and degenerate upon systemic administration of NPA. To experimentally evaluate this hypothesis, we have used adult Wistar rats treated with i.p. injections to administer NPA and kaempferol as an animal model, following the protocol of acute NPA injections and co-administration of a protective kaempferol dose that we established in our previous work [Lagoa et al., 2009].

2. Materials and Methods

2.1. Chemicals

Kaempferol and NPA were supplied by Sigma-Aldrich Spain (Sigma-Aldrich, St. Louis, MO, USA). Glycerol and paraformaldehyde were purchased from Panreac (Barcelona, Spain). Ketamine was from Pfizer (Madrid, Spain). Diazepam and atropine were obtained from B. Braun (Rubí-Barcelona, Spain). All other products were obtained from Sigma-Aldrich or Merck (Darmstadt, Germany) unless specified otherwise.

2.2. Animals and treatments

We followed protocols previously established in our laboratory for the systemic administration of NPA and kaempferol, [Lagoa et al., 2009; Lopez-Sanchez et al., 2020]. Due to this, these protocols are briefly summarized below.

Male Wistar rats, 9–10 weeks old, weighing 290–340 g, were housed in a 12 h light/dark cycle and allowed free access to food and water during the experiment. The experimental procedures followed the animal care guidelines of the European Union Council Directive 86/609/EEC. The protocols were approved by the Ethics Committee for Animal Research of the local government.

The rats were divided into three experimental groups: KNPA, NPA, and Control. The KNPA-group (n = 6) received the first injection of kaempferol solution, at a dose of 21 mg/kg, 48 h before initiation of NPA treatment. From day 0–5 of treatment, a dose of 25 mg of NPA/kg body weight (b.w.) was administered i.p. every 12 h. Daily, 30 min before the morning NPA injection, another 21 mg/kg dose of kaempferol was injected into the rats. Rats from NPA-group (n = 6) were treated with 25 mg NPA/kg b.w. every 12 h during 5 days and, instead of kaempferol, received 1-mL injections with 2.4% v/v DMSO in saline 48 h before NPA-treatment and every day 30 min before the morning NPA injection. Control-group (n = 6) received 1 mL 2.4% v/v DMSO in saline (kaempferol vehicle) and 0.4 mL saline solution (NPA vehicle), with the same time schedule of treatment groups. Systemic administration of NPA at a dose of 25 mg/kg b.w. every 12h caused marked behavioral alterations in the rats, as reported in a previous work [Lagoa et al., 2009].

To avoid a further loss of animals on the fifth day of treatment, the rats in this group with severe pathological symptoms (motor deficit ≥6 or weight loss ≥15%) were sacrificed at the end of day 4. The rats from the KNPA-group, as well as Control-group, were all treated until day 5 and sacrificed at this time.

At the end of the treatments, the animals were anesthetized with ketamine (50 μg/g), diazepam (2.5 μg/g), and atropine (0.05 μg/g). The brains were immediately removed from the skull and washed in cold phosphate-buffered saline (PBS) pH 7.4, and then cut with a tissue slicer. Brain slices without signs of microvessel hemorrhage adjacent to those used for 2,3,5-triphenyl tetrazolium chloride (TTC) staining have been used for all the immunohistochemistry and Western blots shown in this work.

2.3. Motor impairment tests

All the experimental animals were evaluated for motor impairment throughout the experiment. This task was performed as in previous work in this laboratory [Lagoa et al., 2009]. The animals were observed twice a day, just before the i.p. injections of NPA, and rated for the presence and severity of a variety of motor deficits using the quantitative scale described in Ouary et al. (2000). This scale measures gait abnormalities (wobbling gait and paddling), hind limbs dystonia (intermittent or permanent dystonia of one or two hindlimbs), grasping ability with their forepaws to the cage grid for a few seconds, loss of ability to keep equilibrium in a wood platform of 5 × 10 cm and 15 cm height (imbalance test), limb paralysis and recumbency. The maximum score was attributed to a severely affected rat displaying near-death recumbency, unable to grasp the cage grid, and with almost complete hind limb paralysis.

2.4. Brain damage monitored with TTC staining

Staining with TTC was performed as described in previous works in our laboratory [Sun et al., 2005; Lopez-Sanchez et al., 2007; Lagoa et al., 2009].

Coronal 1.5 mm-thick slices of striatum and hippocampus were taken from each of the three experimental groups (KNPA, NPA, and Control), immersed in a 2% solution of TTC in PBS for 15 min at 37°C, and observed under a Leica MZ APO stereomicroscope.

2.5. Brain samples homogenization and Western blotting of C3 and NFκB activation and β-amyloid production

Dissected brain sections of the striatum and hippocampus were immediately frozen in liquid nitrogen. Thereafter, samples were kept at −80°C until use. Samples homogenization and Western blotting were performed as described in detail in a recent publication [Lopez-Sanchez et al., 2020]. Briefly, weighed brain sections were homogenized at 0.14 g per mL in the following ice-cold buffer: 25 mM tris–(hydroxymethyl) aminomethane hydrochloride (Tris-HCl) at pH 7.4, 150 mM NaCl, 5 mM ethylenediaminetetraacetic acid, 50 mM NaF, 5 mM $NaVO_3$ and 4-(1,1,3,3-Tetramethylbutyl)phenyl-polyethylene glycol (Triton X-100) 0.25%, supplemented with the protease inhibitor cocktail SIGMAFAST S8820 (Sigma-Aldrich). After homogenization with a glass homogenizer, 1–1.5 mL aliquots of samples were transferred to an Eppendorf-type plastic vial and sonicated with 30–40 pulses of 100 w of 1 s each using a titanium-tip sonicator in an ice-cold recipient. Afterward, the samples were centrifuged at 2000×*g* for 5 min at 4°C to remove tissue debris and

nuclei, supernatants were collected and their protein concentration was determined with Bradford's method using bovine serum albumin (BSA) as the protein standard. Supernatants were later supplemented with 40% glycerol and conserved at −80ºC until used for Western blotting.

Sodium dodecyl sulfate-polyacrylamide gel electrophoresis (SDS-PAGE) have been performed in a BIO-RAD mini-Protean Tetra cell following a standard protocol with 7.5% acrylamide. Samples were loaded with around 20 μg protein per lane after heat-denaturation of homogenate samples in 95 mM Tris-HCl buffer (pH 6.8), 3% sodium dodecyl sulfate (SDS), 1.5% v/v β-mercaptoethanol, 13% glycerol, and 0.005% bromophenol blue. After SDS-PAGE, the gel was transferred to a polyvinylidene difluoride (PVDF) membrane of 0.2 μm average pore size in standard transfer medium (Trans-BloT TransferMedium, BioRad). Later, PVDF membranes were blocked with 3% BSA, washed 6 times with Tris-buffered saline (TBS) supplemented with 0.05% Triton X-100 (TBST), incubated with the primary antibody against the protein target for 1h at room temperature with shaking. The membranes were washed 6 times with TBST and incubated with the appropriate secondary antibody conjugated with horseradish peroxidase for 1h at room temperature with shaking, washed 6 times with TBST, and treated with Clarity TM Western ECL Substrate, BIO-RAD. Western blots were revealed with Bio-Rad ChemiDocTM XRS+. Primary antibodies used in this work: anti-C3 antibody (Abcam ab200999 –rabbit monoclonal, dilution 1:2,000), anti-NF-κB-p65 polyclonal antibody (Proteintech 10745-1-AP produced in rabbit, dilution 1:1,000), and anti-β-amyloid antibody (Sigma-Aldrich A8354 -mouse monoclonal, at 2 μg/mL). After the acquisition of the PVDF membranes images stained with the primary and corresponding secondary antibodies, membranes were washed with deionized water, stripped, blocked with 3% BSA, and treated to quantify β-actin to monitor protein load as indicated above. To this end, we have used mouse monoclonal anti-β-actin antibody (Sigma-Aldrich A1978, dilution 1:5,000) or polyclonal anti-β-actin antibody produced in rabbit (Sigma-Aldrich A5060, dilution 1:500) as primary antibody, and anti-mouse or anti-rabbit IgG-Horseradish peroxidase (Sigma-Aldrich A0944 and A0545, respectively, dilution of 1:5,000–1:10,000). Of note, we confirmed that after stripping the signal of the staining with the primary antibodies against target proteins C3, NF-κB, and β-amyloid were largely removed and contributed less than 5% to the intensity of the β-actin band.

All the results were confirmed with Western blots of n = 6 different samples of each experimental condition. Statistical analysis: results of Western blots are expressed as means ± standard error of the mean (SEM). Statistical analysis was carried out by Mann–Whitney non-parametric test. A significant difference was accepted at the $p < 0.05$ level.

2.6. Glial fibrillary acidic protein (GFAP), IL-1α, C1q and component C3, TNFα, nuclear factor κB (NF-κB) and neurogranin immunohistochemistry

Dissected brain coronal sections of striatum and hippocampus were embedded in paraffin wax and cut 7 μm thick.

To identify and localize different cells populations we carried out the following immunohistochemistry procedures.

2.6.1. Glial fibrillary acidic protein (GFAP), IL-1α, and C1q

After blocking with 1% BSA for 30 min and incubation with 5% normal goat serum in 1% BSA and 0.1% Triton X-100 for 2h, tissue sections were incubated with primary antibodies: dilution 1:400 for mouse anti-GFAP antibody (Sigma: G3893), and dilution 1:50 for both mouse anti-IL-1α antibody (Santa Cruz Biotechnology: sc-9983) and mouse anti-C1q-C antibody (Santa Cruz Biotechnology: sc-365301). Then, a secondary antibody (dilution 1:200) was added, a goat anti-mouse immunoglobulin G conjugated with alkaline phosphatase (IgG-AP), Santa Cruz Biotechnology: sc-3698. Finally, it was revealed with nitro blue tetrazolium/5-bromo-4-chloro-3-indolyl phosphate (NBT/BCIP) supplied by Roche (catalog nº 1681451).

2.6.2. Complement component 3 (C3), TNFα, NF-κB, and neurogranin

Tissue sections were blocked with endogenous avidin/biotin blocking kit (Abcam ab 64212) and incubated with primary antibodies: dilution 1:2000 for rabbit anti-C3 antibody (Abcam ab225539, a PBS-buffered version of ab200999, containing no BSA or sodium azide), dilution 1:100 for rabbit anti-TNFα antibody (Abcam ab6671), dilution 1:50 for rabbit anti-NF-κB-p65 (Proteintech 10745-1-AP) and dilution 1:500 for rabbit anti-neurogranin (Chemicon AB5620). Sections were incubated with avidin-biotinylated horseradish peroxidase complex (Vectastain ABC Kit). Chromogen development was performed with peroxidase substrate solution (Vector VIP substrate, SK-4600).

2.6.3. Double immunohistochemistry (GFAP + C3; GFAP + NF-κB)

For double immunohistochemistry, primary antibody mouse anti-GFAP was applied together with rabbit anti-C3 or rabbit anti-NF-κB-p65. Secondary antibodies, goat anti-mouse conjugated with alkaline phosphatase and biotinylated goat anti-rabbit Vectastain ABC Kit, were applied together. The chromogen development was performed sequentially as follows: first, anti-GFAP and secondary antibody conjugated with alkaline phosphatase (blue) and, thereafter, the red color was developed with anti-C3 or anti-NF-κB-p65 and a biotinylated secondary antibody conjugated with peroxidase.

2.7. Cell death monitored with terminal deoxynucleotidyl transferase-mediated deoxyuridine triphosphate nick-end labeling (TUNEL) staining

This staining has been performed as in previous work in our laboratory [Sun et al., 2005]. Coronal sections were treated with an *in situ* cell death detection kit, POD (Roche catalog nº 11684817910). Apoptotic cells were identified using a Vector VIP substrate kit (peroxidase detection; Vector Laboratories).

2.8. Image analysis

Quantitative analysis of microscopy images was performed using the Image J® software.

3. Results

3.1. Kaempferol reduces NPA-induced brain degeneration and attenuates NPA-induced neurological deficits

Our results confirmed severe damage in the striatum of rats treated with NPA (NPA-group). Supplementary Fig. 1 shows the lesioned unstained white areas after TTC staining in the regions analyzed in this work. The images shown are representative of those obtained with Control-, NPA- and KNPA-groups. The extent of lesion areas was quantified using Image J® software. The lesion area monitored by TTC staining ranged between 65 and 80% of the striatum in rats of the NPA-group, in good agreement with the results of our previous work [Lagoa et al., 2009]. Tissue damage was not detectable by TTC staining used on rats treated with kaempferol at 21 mg/kg b.w. (KNPA-group). In the hippocampus is observed a weaker TTC staining in NPA-group relative to Control and KNPA-group.

The protection effect of kaempferol against NPA-induced damage in the striatum, the brain region most affected by NPA [Brouillet et al., 2005; Lagoa et al., 2009], was further assessed using neurogranin staining, a neuronal marker [Represa et al., 1990], and TUNEL assay, an apoptotic marker [Cheng et al., 2002]). Immunolabeling with neurogranin of coronal striatum sections revealed tissue degeneration, see the lighter stained areas in rats from NPA-group (Supplementary Fig. 2A), with a similar regionalization to the one observed with TTC staining (Supplementary Fig. 1), revealing a very significant loss of staining with respect to the area surrounding the lesion core. The higher

magnification images of the lesion core and surrounding areas shown in Supplementary Fig. 2A also reveal a large loss of cells and disruption of the compact tissue structure in the lesion core of rats of the NPA-group. In addition, the observed extensive TUNEL labeling in the lesion core of the striatum is indicative of widespread cell death, with remarkably lower TUNEL labeling in the area surrounding the core (Supplementary Fig. 2B). A high magnification detail showing one labeled neuron is included in the green square of the NPA-group image of the lesion core to highlight nuclear labeling. Sections of brains from Control- and KNPA-groups do not show significant TUNEL labeling.

All experimental animals were evaluated for motor impairment throughout the experiment as described in the Materials and Methods. Systemic administration of NPA at a dose of 25 mg/kg b.w. every 12h caused marked behavioral alterations in the rats, in agreement with previous reports [Ouary et al., 2000; Lagoa et al., 2009; Ren et al., 2019]. After the first and second NPA injections, the animals showed reduced reactive activity during handlings relative to control animals, although maintaining a normal posture and gait. Through days 2 and 3, the animals showed dystonic movements of hind limbs and wobbling gait and paddling. On the 4th day, the animals lost grasping ability and balance capacity. By days 4–5, the rats became recumbent, with progressive limbs paralysis and a dying appearance. Our results show that the administration of kaempferol drastically reduced the neurological disorders induced by NPA.

3.2. *Kaempferol prevents the increase of complement C3 protein expression and activation, a reactive A1 astrocyte marker in NPA-induced brain damage*

Brain samples were excised from 1.5 mm thick brain slices neighboring TTC-stained slices (Supplementary Fig. S1) and homogenized as indicated in the Materials and Methods.

Western blots revealed that C3α levels in the striatum and hippocampus strongly increased in rats of the NPA-group relative to the Control-group, namely 4,44 ± 0.4 and 5,9 ± 0.5 -fold, respectively (Fig. 1 and Supplementary Fig. S3). In addition, these results also revealed enhanced proteolytic processing of C3α in rats of the NPA-group leading to lower molecular weight fragments, i.e. C3 protein activation. Of note, in the striatum and hippocampus, this increase is much higher if the increase is calculated from the sum of the C3α and all C3α fragments detected by the anti-C3 antibody used in this work for Western blotting (Abcam, ab200999). Thus, these results suggested an enhanced generation of reactive A1 astrocytes in the striatum and hippocampus, the brain areas that have been shown in many studies to be more prone to NPA-induced degeneration. Indeed, no significant increase of C3α and all C3α fragments can be seen in the brain stem of rats of the NPA-group relative to rats of the Control-group (*data not shown*).

In addition, the results shown in Fig. 1 demonstrated that the increase of the C3α was statistically non-significant ($p > 0.05$) in the striatum and hippocampus of rats treated with kaempferol and NPA (KNPA group). The same result was obtained if the calculations are performed from the sum of C3α plus all the C3α fragments, instead of only the C3α expression level.

3.3. *Immunohistochemical analysis of the regionalization and location of complement C3 protein and major proteolytic fragments show that kaempferol also protects against reactive A1 astrocytes induction in Wistar rat's brain by acute i.p. NPA treatment*

Through immunohistochemical analysis, we have studied the location and regionalization of complement C3 protein in brain coronal sections. Since the manufacturer indicates that the anti-C3α antibody used in this work can also bind to blood plasma components, this point was experimentally assessed using excised rat brain slices of the NPA-group [Supplementary Fig. S4]. Despite that in all this work we have taken special care to use immunohistochemistry brain slices not showing

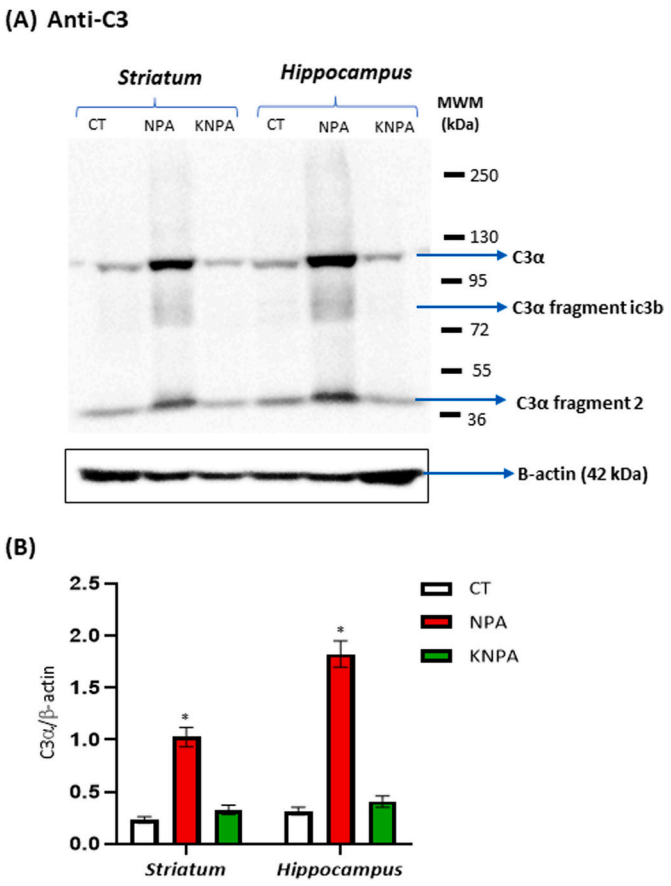

Fig. 1. Kaempferol i.p. administration protects against the increase of C3α and C3α proteolytic fragments induced by i.p. administration of NPA in the striatum and hippocampus with respect to rats of the Control-group. (A) Representative Western blot of C3 protein and β-actin of striatum and hippocampus homogenates of rats of Control-group (CT), NPA-group (NPA), and KNPA-group (KNPA). After the acquisition of images of the Western blot with anti-C3 antibody, the PVDF membrane was stripped and processed for the Western blot of anti-β-actin, as indicated in the Materials and Methods. The β-actin band has been cropped from Supplementary Fig. S3 included at the end of this manuscript. The molecular weights of the protein markers (MWM) are indicated on the right-hand side. (B) A plot of the ratio of (C3α/β-actin) in striatum and hippocampus homogenates of rats of CT-, NPA- and KNPA-groups. The bars are the means ± SEM of the results obtained with samples of each group of rats (n = 6). (*) $p < 0.05$ relative to control rats.

signs of a significant micro-hemorrhage in the observation area, small thin lines observed in some of the images are likely fingerprints of capillaries.

As activation of C3 protein has earlier been identified as a reactive A1 astrocyte marker [Liddelow et al., 2017; Lopez-Sanchez et al., 2020], we identified both C3 protein and GFAP using double immunochemistry in NPA-group (Fig. 2A and B). Immunostaining with anti-C3α and anti-GFAP is revealed by red and blue colors, respectively. The localization and distribution of pixels stained in blue and red in the low magnification images of Fig. 2A and B can be better seen in Supplementary Fig. S5, which shows the overlay of blue and red channel images obtained using Image J software as indicated in the Materials and Methods section. Our results show high C3 immunostaining in the lesion core, overlapping with the necrotic area, labeling cellular somas. However, ameboid-shape reactive A1 astrocytes are hardly seen in this largely degraded lesion core, a result that is consistent with the large drop of astrogliosis in this area indicated by the results of GFAP immunostaining. On the other hand, we observed high C3 immunolabeling in the area surrounding the core but, in this area, double

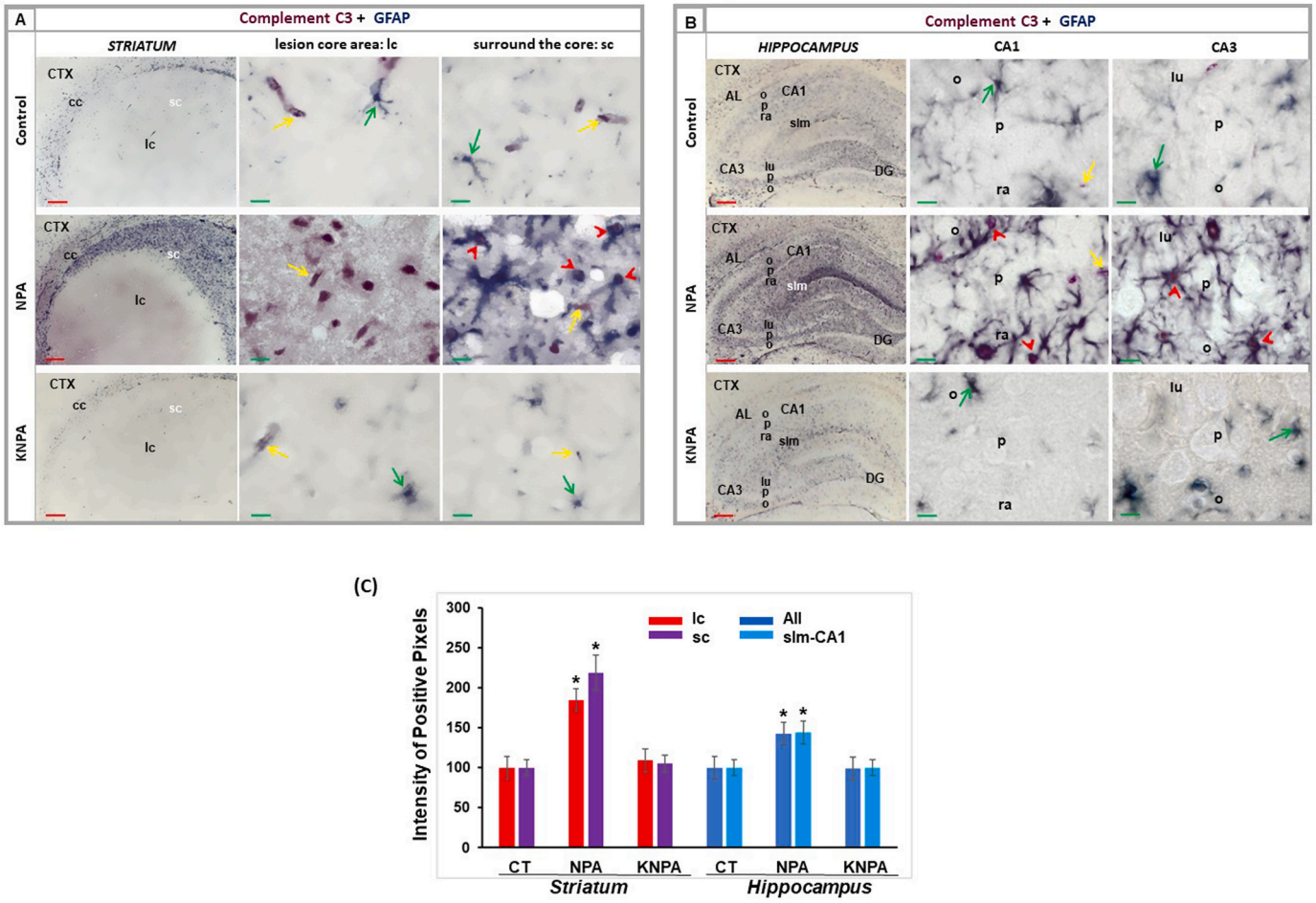

Fig. 2. Double immunohistochemistry with anti-C3 (in red) and anti-GFAP (in blue) antibodies in the striatum (A) and hippocampus (B) in the brain coronal sections prepared from Control-, NPA- and KNPA-groups. In NPA-group, note C3 immunostaining in the cellular somas of the lesion core (lc) in the striatum (A). In contrast, in the area surrounding the core (sc) in the striatum (A), ameboid-shape reactive A1 astrocytes (red arrowheads) show a co-location of C3 and GFAP, also observed (red arrowheads) in CA1 as well as CA3 (Ammon's horn) fields in the hippocampus (B). Co-location of complement C3 and GFAP is not observed in Control- and KNPA-groups. As a significant characteristic of anti-C3 antibody, small blood vessels are marked in the three groups (yellow arrows). Abbreviations used in this Figure: AL, alveus; cc, corpus callosum; CTX, Cerebral cortex; DG, dentate gyrus; lu, stratum lucidum; o, stratum oriens; p, pyramidal layer; ra, stratum radiatum; slm, stratum lacunosum-moleculare. Green arrows: astrocytes. Red scale bars: 200 μm. Green scale bars: 10 μm. (C) Histograms of the intensity of positive pixels of the images of C3 staining were obtained with Image J® software for n = 3 different rats of each group. Positive pixels mean pixels with an intensity higher than 80% of the saturation value and the average intensity shown is the normalized value (100% for controls). Rat brain sections treated with kaempferol (KNPA-group) show a low immunoreactivity, similar to the Control-group. (*) $p < 0.05$ with respect to Control-group. (For interpretation of the references to color in this figure legend, the reader is referred to the Web version of this article.)

immunohistochemistry revealed co-location of C3 and GFAP in the ameboid-shape reactive A1 astrocytes (Fig. 2A). Similarly, our results show co-location of C3 and GFAP in the ameboid-shape reactive A1 astrocytes located in the hippocampus (Fig. 2B), intensively observed in CA1 and CA3 areas and the vicinal dentate gyrus.

Histograms of the average counts of pixels with high intensity of the images of C3α staining obtained from different rats of each group are shown in Fig. 2C. The quantification of high-intensity pixels points out that the average increase is 1.85- and 2.2-fold in the lesion core and the surrounding area of the striatum, respectively, and 1.45-fold in the hippocampus.

This increase of distribution and regionalization of complement C3 protein expression, as well as the presence of reactive A1 astrocytes, detected in the NPA-group, is fully prevented in rats treated with kaempferol and NPA (KNPA-group) in the regions analyzed, which shows an immunostaining pattern very similar to the Control-group of rats (Fig. 2A and B).

3.4. Kaempferol prevents the increase of pro-inflammatory cytokines IL-1α, TNFα, and complement C1q in the striatum and hippocampus of NPA-treated rats

As shown in a recent publication of our laboratory [Lopez-Sanchez et al., 2020], the treatment with NPA also induces increased levels of the proinflammatory cytokines IL-1α and TNFα, and C1q in the brain regions of Wistar rats that generate reactive A1 astrocytes. It has been shown by other investigators that these cytokines are secreted by activated microglia and induce neurotoxic A1 astrocytes [Zhang et al., 2014; Bennett et al., 2016; Liddelow et al., 2017]. A careful selection of brain slices with low capillarity is also of relevance here, since Supplementary Fig. S4 shows the unspecific staining of the blood plasma with anti-complement C3, anti-IL-1α, and anti-C1q antibodies (yellow arrows), in good agreement with the indications of the manufacturers.

Immunostaining with specific antibodies reveals the increase of IL-1α, TNFα, and C1q in striatum brain slices of rats of the NPA-group relative to the Control-group (Fig. 3A). More than a two-fold increase can be calculated for the cytokines IL-1α and TNFα, and complement C1q from cell counting of selected higher magnification images.

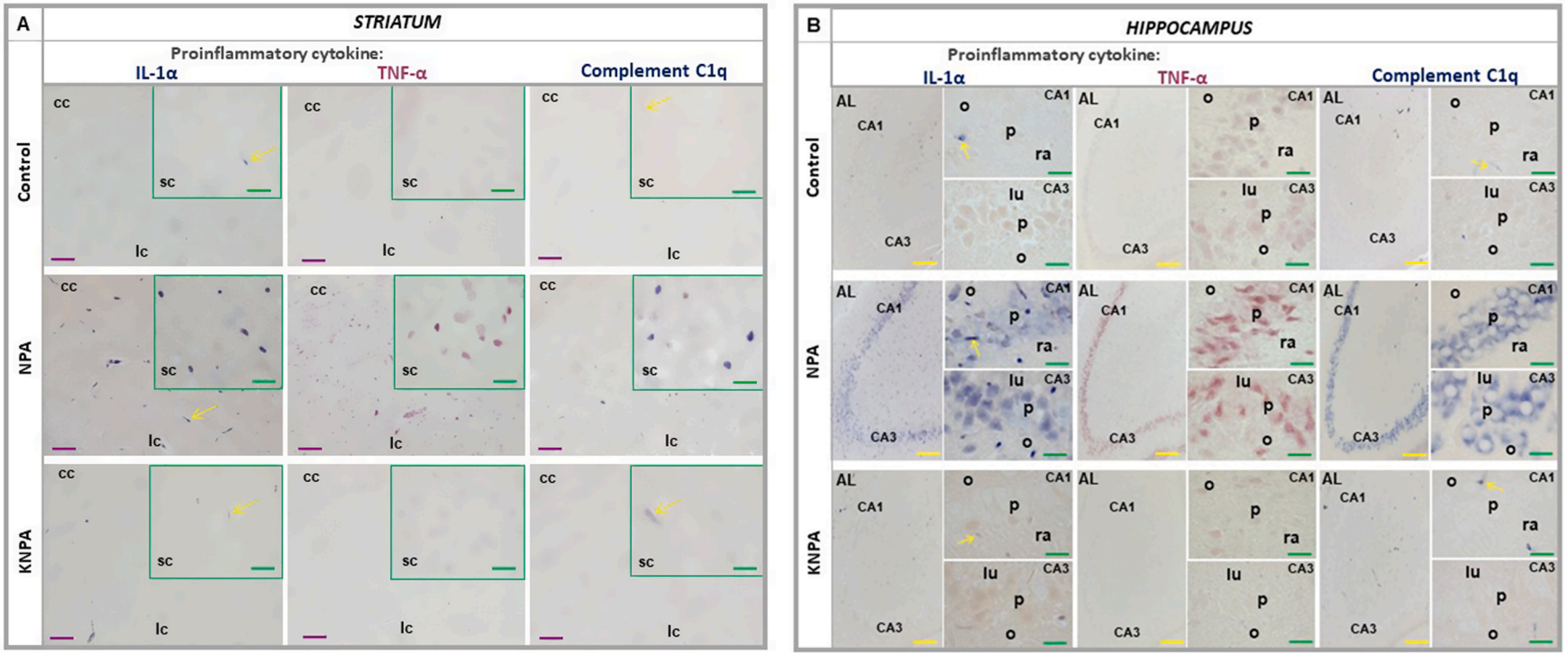

Fig. 3. Kaempferol prevents an increase in proinflammatory cytokines IL-1α, TNFα, and complement C1q in the striatum (A) and the hippocampus (B) of NPA-treated rats. (A) Representative coronal sections of the striatum (A) and hippocampus (B) after immunohistochemistry with anti-IL-1α, anti-TNFα, and anti-C1q antibodies corresponding to Control-, NPA- and KNPA-groups. In the NPA-group the cellular somas are stained in the area surrounding the core (sc) in the striatum (A), and in CA1 and CA3 (Ammon's horn) fields in the hippocampus (B). Brain sections of rats treated with kaempferol (KNPA-group) show a low immunoreactivity, similar to the Control-group. No staining in the cellular soma is observed in Control- and KNPA-groups. As a significant characteristic of anti-IL-1α and anti-C1q antibodies, small blood vessels are marked in the three groups (yellow arrows). Abbreviations used in this Figure: AL, alveus; cc, corpus callosum; lc, lesion core area; lu, stratum lucidum; o, stratum oriens; p, pyramidal layer; ra, stratum radiatum. Yellow scale bars: 100 μm. Purple scale bars: 50 μm. Green scale bars: 10 μm. (For interpretation of the references to color in this figure legend, the reader is referred to the Web version of this article.)

The frames with higher magnification in Fig. 3A point out the strong staining of cell bodies by these cytokines and the small apparent particle size of the cells heavily stained with TNFα is consistent with the known nuclear translocation of this cytokine. In addition, the striatum brain slices prepared from the KNPA-group display a pattern of immunostaining with the cytokines and complement C1q that is not significantly different from Control-group for C1q and TNFα, and at most 20% higher for IL-1α (Fig. 3A).

The results obtained with hippocampus slices also show that NPA treatment increases the expression of these cytokines and complement protein C1q in this brain area and that this is fully prevented by co-administration of kaempferol at the doses that prevent C3α activation (Fig. 3B). Immunostaining of hippocampus slices with anti-IL-1α, anti-TNFα, and anti-C1q point out that NPA treatment induced a large increase of these cytokines in the Ammon's horn CA1 and CA3 regions, heavily staining the soma of pyramidal neurons. Note that this is not seen in the hippocampus slices prepared from the KNPA-group, whose immunostaining pattern is not significantly different from those of rats of the control group.

3.5. Kaempferol prevents the NPA-induced increase of NF-κB expression in the striatum and hippocampus

Next, we have experimentally assessed whether kaempferol co-administration can prevent the NPA-induced rise of NF-κB expression because activation of NF-κB has been shown to take place in NPA-induced brain neurodegeneration [Ryu et al., 2003; Chakraborty et al., 2014; Jin et al., 2018] and this is a molecular mechanism underlying the enhanced expression of many cytokines [Gutierrez-Merino et al., 2011]. Western blots revealed that NF-κB-p65 levels in the striatum and hippocampus increased in rats of the NPA-group relative to the Control-group, and also that this increase was fully prevented by co-administration of kaempferol at the doses that prevented C3α activation (Fig. 4).

These results were confirmed by using immunohistochemistry in coronal slices of the striatum and hippocampus (Fig. 5). In the striatum of the NPA-group (Fig. 5A), no staining in cellular somas is observed in the lesion core, which is consistent with the advanced tissue damage revealed by TTC staining, as pointed out in previous work [Lagoa et al., 2009] and also in the Supplementary Fig. S1. In contrast, in the area surrounding the lesion core of the striatum, we observe a co-location of NF-κB-p65 and GFAP in ameboid-shape reactive astrocytes (Fig. 5A), in good agreement with our immunohistochemistry results obtained with anti-C3α reactive astrocytes staining (Fig. 2A). In the hippocampus, TTC staining does not reveal extensive damage in NPA-treated rats (Supplementary Fig. S1). However, our immunohistochemistry analyses (Fig. 5B) demonstrate that NPA treatment also elicits a co-location of NF-κB-p65 and GFAP in ameboid-shape reactive astrocytes (labeled with red-arrowheads) in CA1 and CA3 fields of the hippocampus.

Our findings demonstrate that kaempferol, at the doses that prevented C3α activation (Fig. 2), prevents the appearance of reactive astrocytes marker NF-κB-p65 staining (Fig. 5). Nevertheless, in the hippocampus NF-κB-p65 immunostaining remains restricted to neuronal soma of CA1 and CA3 pyramidal neurons in the KNPA-group, like in Control-group (Fig. 5B). It is to be recalled that high basal constitutive NF-kB activity was found in glutamatergic neurons of the CNS, such as the hippocampus granule cells and CA1 and CA3 pyramidal neurons [Kaltschmidt et al., 1994, 1995].

3.6. Kaempferol protects against the increase of amyloid β peptides production in the hippocampus and striatum of NPA-treated rats

Since it has been shown that reactive astrocytes can generate neurotoxic amyloid β peptides [Nadler et al., 2008; Zhao et al., 2011; Frost and Li, 2017], we decided to experimentally assess whether astroglia activation leads to increased production of amyloid β peptides

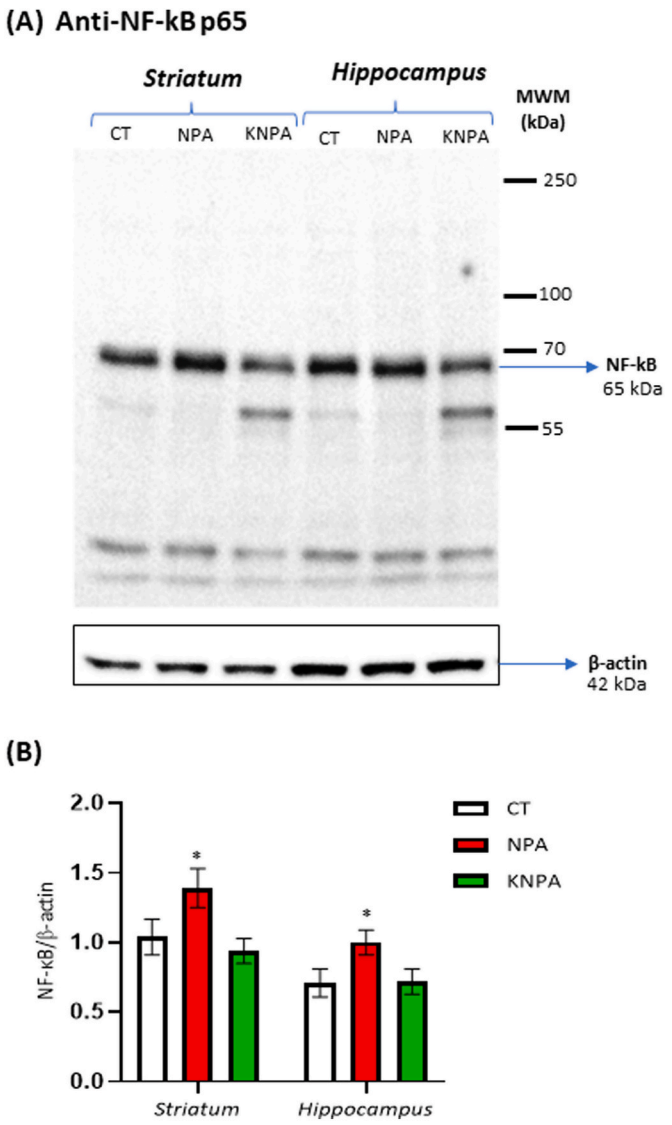

Fig. 4. Kaempferol co-administration prevents the increase in NF-κB induced by NPA treatment. (A) Representative Western blot of NF-κB and β-actin of striatum and hippocampus homogenates of rats of Control-group (CT), NPA-group (NPA), and KNPA-group (KNPA). After the acquisition of images of the Western blot with anti-NF-κB-p65 antibody, the PVDF membrane was stripped and processed for the Western blot of anti-β-actin, as indicated in the Materials and Methods. The β-actin band has been cropped from Supplementary Fig. S3 included at the end of this manuscript. The molecular weights of the protein markers (MWM) are indicated on the right-hand side. (B) A plot of the ratio of (NF-κB/β-actin) in striatum and hippocampus homogenates of rats of CT-, NPA- and KNPA-groups. The bars are the means ± SEM of the results obtained with samples of each group of rats (n = 6). (*) $p < 0.05$ relative to Control rats.

in the striatum and hippocampus during NPA-induced brain neurodegeneration. The results of Western blots of homogenates of striatum and hippocampus slices stained with anti-amyloid β peptides of rats of control, NPA-treated, and KNPA-treated groups are shown in Fig. 6. Fig. 6B shows the analysis of the ratio C99-cleavage fragment of APP/β-actin, but a similar trend can be seen in the protein bands corresponding to smaller size amyloid β peptides, bands between 35 and 50 kDa, and peptides of less than 15 kDa migrating near the front of the gel. These results demonstrated that treatment with NPA induces amyloid β peptides production in both brain areas and, also, that co-administration of kaempferol at the doses that prevent C3α activation completely protects against the increase of amyloid β peptides production induced by i.p. treatment of rats with NPA.

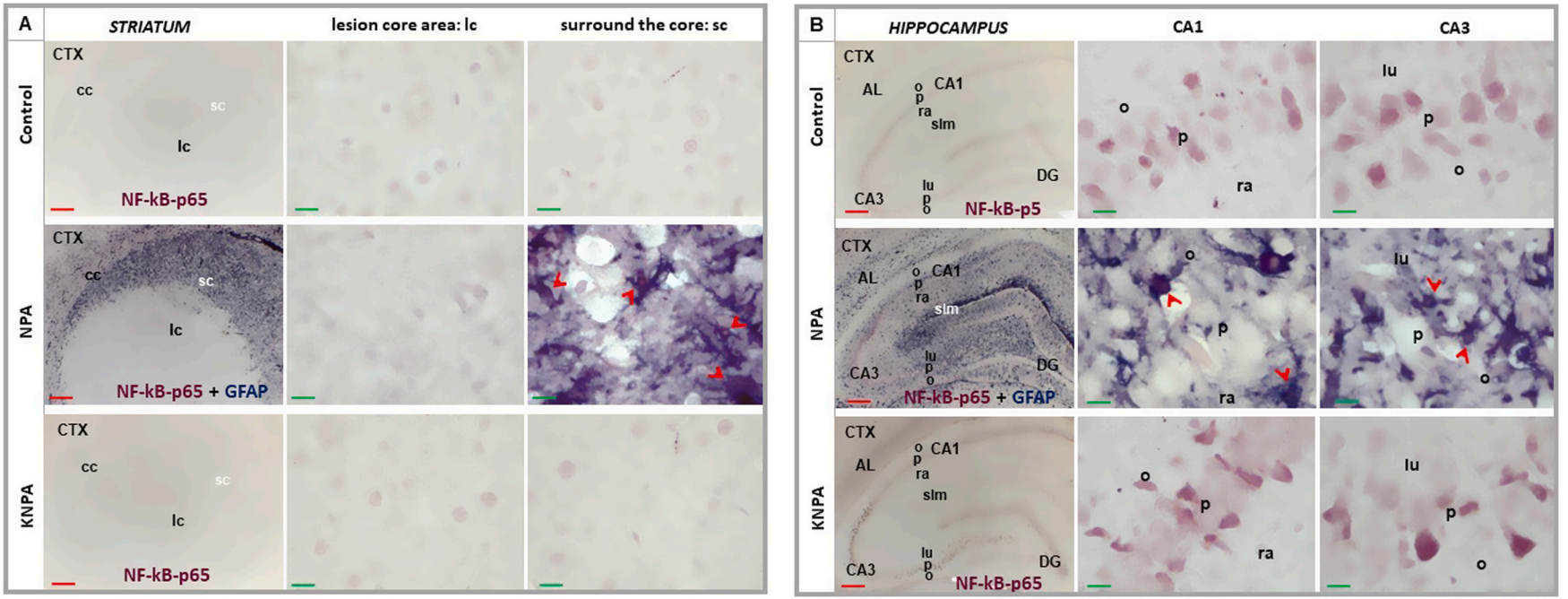

Fig. 5. Representative coronal sections of the striatum (A) and hippocampus (B). Immunohistochemistry with anti-NF-κB-p65 (in red) of Control- and KNPA-groups. Double immunohistochemistry with anti-NF-κB-p65 (in red) and anti-GFAP (in blue) antibodies in the NPA group. In NPA-group, note the co-location of NF-κB-p65 and GFAP in ameboid-shape reactive A1 astrocytes (red arrowheads) in the area surrounding the core (sc) in the striatum (A) and, also, in CA1 and CA3 (Ammon's horn) fields in the hippocampus (B). In the lesion core area (lc) of the striatum (A) no staining in cellular somas is observed with NF-κB-p65 in Control-, NPA-, and KNPA-groups. In contrast, in the hippocampus (B) pyramidal neurons (p) of CA1 and CA3 show staining with NF-κB-p65 in Control-and KNPA-groups. AL: alveus; cc: corpus callosum; CTX: Cerebral *cortex*; DG: dentate gyrus; lu: stratum lucidum; o: stratum oriens; ra: stratum radiatum. Red scale bars: 200 μm. Green scale bars: 10 μm. (For interpretation of the references to color in this figure legend, the reader is referred to the Web version of this article.)

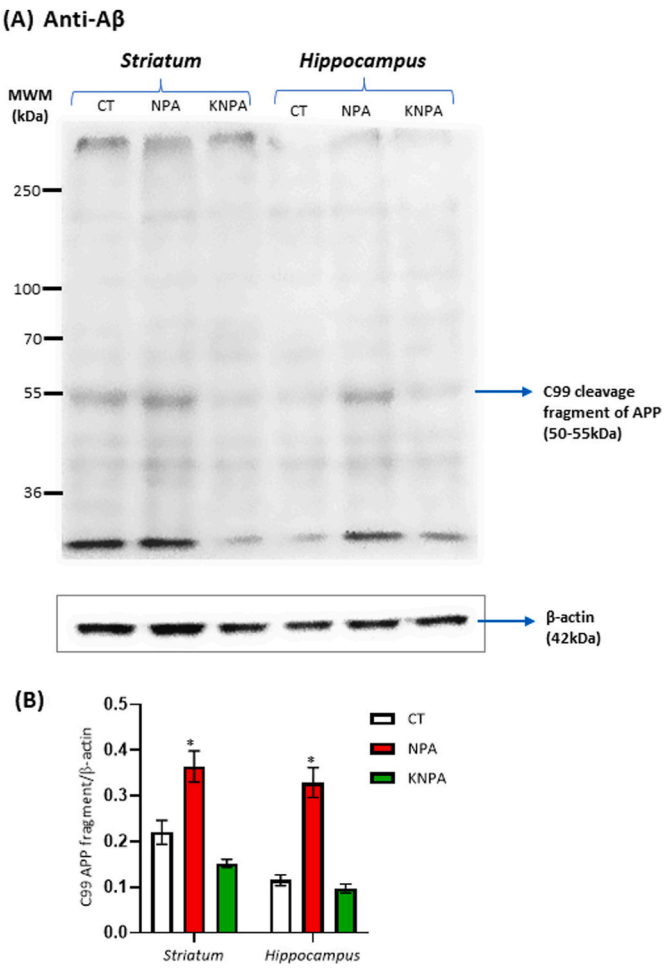

Fig. 6. Kaempferol co-administration prevents the increase in amyloid β peptides induced by NPA treatment. (A) Representative Western blot of amyloid β peptides and β-actin of striatum and hippocampus homogenates of rats of Control-group (CT), NPA-group (NPA), and KNPA-group (KNPA). After the acquisition of images of the Western blot with anti-β-amyloid antibody, the PVDF membrane was stripped and processed for the Western blot of anti-β-actin, as indicated in the Materials and Methods. The β-actin band has been cropped from Supplementary Fig. S3 included at the end of this manuscript. The molecular weights of the protein markers (MWM) are indicated on the left-hand side. (B) A plot of the ratio of (C99 cleavage fragment of APP of 50–55 kDa/β-actin) in striatum and hippocampus homogenates of rats of CT-, NPA-, and KNPA-groups. The bars are the means ± SEM of the results obtained with samples of each group of rats (n = 6). (*) $p < 0.05$ relative to Control rats.

4. Discussion

The major result of this work is the protection against proteolytic activation of complement C3 protein by i.p. administration of kaempferol at a dose that also protects efficiently against the rise of markers of neurodegeneration and against the neurological dysfunctions induced by acute i.p. injections of the neurotoxin NPA in male adult Wistar rats, as shown by the good neurological scores of the rats of the KNPA-group, which are in good agreement with those reported in earlier work [Lagoa et al., 2009]. To the best of our knowledge, this is a novel finding not previously reported elsewhere. The kaempferol dose used to perform this work, 21 mg/kg b.w., was chosen based on a previous study of our laboratory with this experimental model of i.p. injections of NPA [Lagoa et al., 2009]. Lower doses of kaempferol afforded only partial protection against striatum degeneration [Lagoa et al., 2009]. Also, it is to be noted that herbal extracts of *Persicaria lapathifolia* that contains kaempferol glycoside are inhibitors of the classical pathway of complement C3 protein activation [Park et al., 1999]. The results of this work show that i.p. administration of kaempferol results in an almost complete blockade of the NPA-induced increase of C3α and other proteolytic fragments of C3 (iC3b, C3α fragment 2, and lower molecular weight fragments) in the brain regions studied, i.e. striatum and hippocampus. Of note, in a recent study, we have shown that a rise in C3α levels is an early event in NPA neurotoxicity that precedes the appearance of severe neurological dysfunctions [Lopez-Sanchez et al., 2020]. Taking into account that the TTC staining of brain slices of rats of the NPA-group shows large differences between the extent of damage in the striatum and the hippocampus, this result by itself points out that kaempferol bears a large therapeutic potential to protect against NPA-induced brain degeneration in major brain regions affected by this neurotoxin. Indeed, histochemical results lend further support to this conclusion, since the levels of tissue markers of NPA-induced brain neuroinflammation (C3 activation, NF-κB immunostaining, astrogliosis, pro-inflammatory cytokines IL-1α and TNFα, and C1q) and neurodegeneration (TTC staining and TUNEL labeling), in striatum and hippocampus slices from rats of the KNPA-group are similar to those found in the slices of these brain areas from the Control-group, this work and our previous work [Lagoa et al., 2009].

The histochemical studies included in this work also revealed that C3α immunostaining in the brain shows a remarkable regional and cellular pattern after i.p. injections with acute NPA doses leading to neurological dysfunctions that mimic those found in Huntington's disease. Li et al. (2019) have reported that neurons showing signs of degeneration are marked by upregulated proteins C3 and C1q and are surrounded by activated microglia. In the striatum, the brain region undergoing the more extensive damage according to our TTC staining results, the immunostaining with anti-C3 antibody is largely enhanced not only in the necrotic area visualized with TTC staining, but also in the vicinal cortical and striatum areas surrounding the lesion core. Indeed, the anti-C3 antibody immunostaining is more intense in these latter vicinal areas, as expected due to the extensive cell loss and tissue degradation observed in the lesion core in this work, accompanied by a significant loss of protein mass as shown in previous work [Lagoa et al., 2009]. As we have shown in a recent work [Lopez-Sanchez et al., 2020], in the early stages of NPA-induced neurotoxicity the immunostaining pattern observed with anti-C3 antibody in the striatum slices of rats of the NPA group closely mimics the immunostaining pattern observed with the glial marker anti-GFAP antibody, which revealed astrogliosis. In this work, at an advanced stage of NPA-induced striatum degeneration, double immunostaining with anti-C3 and anti-GFAP antibodies showed their co-localization in ameboid-shape astrocytes mostly in areas surrounding the lesion core of the striatum in this work, likely because most reactive A1 astrocytes have been already degraded in the lesion core. However, secreted activated C3, a specific marker of these neurotoxic astrocytes [Liddelow et al., 2017], seems to remain high in the lesion core of the striatum for some time after A1 astrocytes are degraded, becoming a fingerprint of an earlier generation of these type of astrocytes. Furthermore, this conclusion is also supported by the similarity between immunostaining patterns obtained with anti-TNFα, anti-IL-1α, and anti-C1q antibodies, because these cytokines secreted by activated microglia are known to foster reactive A1 astrocytes generation [Liddelow et al., 2017]. The immunostaining patterns of C3, GFAP, IL-1α, C1q, and TNFα antibodies obtained with striatum slices of the rats of the KNPA-group are not significantly or only weakly different from those obtained with striatum slices of the rats of the Control-group. Therefore, we can conclude that i.p. administration of kaempferol at the dose used in this work prevents efficiently the activation of complement C3 protein and generation of reactive A1 astrocytes induced by acute treatment with NPA in the striatum. In addition, our results show that kaempferol also prevented microglia activation in NPA-induced brain degeneration, as previously reported by other publications [Ryu et al., 2003; Chakraborty et al., 2014; Jin et al., 2018].

In previous work, we have shown that induction of reactive A1

astrocytes by i.p. NPA administration is an early event in NPA neurotoxicity that takes place not only in the striatum but also in the hippocampus [Lopez-Sanchez et al., 2020]. It is to be recalled here that systemic NPA administration to rodents has been shown to produce memory impairment [Browne et al., 1999; Menze et al., 2015]. The immunohistochemical results obtained in this work with slices of the hippocampus of rats of the NPA-group show the presence of A1 astrocytes in CA1 and CA3 hippocampal regions and the vicinal dentate gyrus area. We wish to note that the anti-C3 antibody used in this work will give positive immunostaining of all types of cells expressing C3α or C3α-derived fragments or their corresponding complement receptors bound to these C3 fragments, which are transmembrane proteins anchored at the cell surface [Li et al., 2011]. In addition, other proteases like extracellular metalloproteinases and cathepsins, which are activated in brain neurodegeneration [Rosenberg, 2009; Nakanishi, 2020], can act as auxiliary proteases in the proteolytic processing of C3 [Huber-Lang et al., 2018]. Indeed, C3 expression has been reported in experimental models of neuronal apoptotic cells [Thomas et al., 2000; Morita et al., 2006; Hernandez-Encinas et al., 2016]. In contrast, the weak immunostaining with anti-C3, anti-IL-1α, anti-C1q and anti-TNFα antibodies found in the hippocampus slices from rats of the KNPA-group is not significantly different from that found in slices from rats of the Control-group. Therefore, we can conclude that i.p. administration of kaempferol also prevents efficiently the activation of complement C3 protein and generation of reactive A1 astrocytes induced by acute treatment with NPA in the striatum and the hippocampus.

In previous work, we showed that i.p. co-administration of 21 mg of kaempferol/kg b.w. largely prevents the rise of cellular oxidative stress markers in NPA-induced brain degeneration [Lagoa et al., 2009]. In this work, we show that i.p. co-administration of this dose of kaempferol fully prevents the rise of the expression of NF-κB in the striatum and the hippocampus of NPA-treated rats. In earlier works, it has been shown that NF-κB activation mediates the secretion of microglial pro-inflammatory cytokines that mediate NPA-induced brain degeneration [Ryu et al., 2003; Chakraborty et al., 2014; Jin et al., 2018]. Therefore, our results lend support to the hypothesis that the activation of the NF-κB signaling pathway by cellular oxidative stress is the major molecular mechanism underlying the enhanced production of pro-inflammatory cytokines, IL-1α and TNFα, and C1q in NPA-induced degeneration of the striatum and the hippocampus. On these grounds, it seems that kaempferol inhibition of microglial activation can, at least in part, account for its protective effects against NPA-induced brain degeneration. However, the putative implication of other cellular stress signaling pathways in the production of these cytokines cannot be excluded in poisoning by neurotoxins, see for example [Wang et al., 2021]. In addition, Wang et al. (2021) showed that reactive astrocytes can also further potentiate the activation of microglia. Reactive astrocytes-dependent activation of microglia is likely to afford a major contribution to spreading the neuronal damage within the initially affected brain areas and, also, to peripheral neuronal structures. Since kaempferol blocked reactive A1 astrocytes generation, this feed-forward harmful cycle is, also, blocked by kaempferol in the striatum and in the hippocampus. Thus, the molecular mechanisms of the blockade by kaempferol of reactive A1 astrocyte generation and microglia activation in the rat brain induced by i.p. administration of NPA deserve to be further investigated. Nevertheless, the results reported in this work reveal a potential novel therapeutic use of this flavonoid, because induction of neurotoxic reactive A1 astrocytes has been found in post-mortem samples of many human neurodegenerative diseases, like Alzheimer's, Parkinson's, and Huntington's diseases, and in amyotrophic lateral sclerosis and multiple sclerosis [Liddelow et al., 2017]. Indeed, Stanek et al. (2019) using the YAC128 mouse model have suggested that astrocyte dysfunction may play a critical role in Huntington's disease pathogenesis, although this is still a controversial point because it has been questioned by other authors using other mouse models [Diaz-Castro et al., 2019]. The effective doses of kaempferol that afford protection against activation of complement C3 protein in the brain are likely to be strongly dependent upon the administration route of this flavonoid. Indeed, we showed that intravenous injections of only 100–200 μM of kaempferol in the blood produce extensive protection against the striatal neurodegeneration caused by transient focal cerebral ischemia induced by middle cerebral artery occlusion in adult rats [Lopez-Sanchez et al., 2007]. For comparison, the amount of kaempferol used for intravenous injections in Lopez-Sanchez et al. (2007) was 0.16–0.25 mg of kaempferol/kg b.w., while i.p. injections used in this work have been 21 mg of kaempferol/kg b.w.

Finally, in this work, we found an increase of amyloid β peptides in the striatum and a higher increase in the hippocampus of NPA-treated rats. To the best of our knowledge, this is a novel finding in NPA-induced brain neurodegeneration and it has special relevance because exposure to NPA has been recently shown to induce tau pathology in the tangle-mouse model and also in wildtype-mice [Lahiani-Cohen et al., 2020]. Neurofibrillary tangles of tau and amyloid β peptides are major hallmarks in Alzheimer's disease, a neurodegenerative disease in which the generation of reactive A1 astrocytes has also been reported [Liddelow et al., 2017]. Therefore, the NPA-induced neurodegenerative process shares these molecular biomarkers with Alzheimer's disease. Also, our results show that co-administration of kaempferol prevents the increase of amyloid β peptides induced by NPA. Interestingly, Babaei et al. (2021) have recently reported that i.p. administration of kaempferol at 10 mg/kg b. w. for 21 days affords cognitive improvement in a mouse model of sporadic Alzheimer's disease. In another recent study performed with a mice model of Parkinson's disease, Han et al. (2021) administered 50 mg/kg b. w of kaempferol by i.p. injection to experimentally assess the protective effect of this natural compound. Gao et al. (2019) have evaluated the anti-depressive effect of kaempferol by using 10 and 20 mg/kg b. w. in an animal model of chronic social defeat stress. Therefore, the dose of kaempferol used in this work (21 mg/kg b. w.) is within the range of doses used in all these studies performed in animal models that mimic neurodegenerative or depressive disorders. In spite that reactive astrocytes can produce neurotoxic amyloid β peptides [Nadler et al., 2008; Zhao et al., 2011; Frost and Li, 2017], further experimental work is still needed to demonstrate whether kaempferol inhibits the generation of reactive astrocytes directly or indirectly through inhibition of microglia activation. Yet, the putative beneficial effects of kaempferol in Alzheimer's disease are a pending issue, although clinical trials have reported improvements in cognitive function and memory impairment from treatment with the flavonoid-rich *Ginkgo biloba* extract [Praticò and Delanty, 2000; Ward et al. 2002], which contains kaempferol.

In conclusion, i.p. administration of daily doses of 21 mg of kaempferol/kg b.w. prevents efficiently against the proteolytic activation of complement C3 protein and generation of reactive A1 astrocytes induced by acute treatment of adult Wistar rats with NPA in the brain regions studied in this work, i.e. striatum and hippocampus. This action of kaempferol correlates with its ability to afford protection against NPA-induced neurodegeneration of these brain areas. Kaempferol also blocks the activation of the NF-κB signaling pathway, suggesting that this is the major molecular mechanism inducing the enhanced secretion of cytokines IL-1α and TNFα, and of C1q that elicits the generation of reactive A1 astrocytes in the rat model used in this work. In addition, enhanced production of amyloid β peptides has been found in NPA-induced brain degeneration, which is also prevented by kaempferol administration. Thus, this work highlights novel biological roles of this antioxidant flavonoid. The inhibition by kaempferol of C3 proteolytic activation in the brain suggests a potential novel therapeutic use of this flavonoid because induction of neurotoxic reactive A1 astrocytes has been found in post-mortem samples of many human neurodegenerative diseases.

CRediT authorship contribution statement

Carmen Lopez-Sanchez: Conceptualization, Data curation, Formal analysis, Investigation, all authors, Methodology, Supervision, Writing – original draft, Writing – review & editing. **Joana Poejo:** Data curation, Formal analysis, Investigation, all authors, Methodology, Writing – original draft, Writing – review & editing. **Virginio Garcia-Lopez:** Data curation. **Jairo Salazar:** Data curation. **Virginio Garcia-Martinez:** Conceptualization, Funding acquisition, Formal analysis, Investigation, all authors, Methodology, Supervision, Writing – original draft, Writing – review & editing. **Carlos Gutierrez-Merino:** Conceptualization, Formal analysis, Funding acquisition, Investigation, all authors, Methodology, Supervision, Writing – original draft, Writing – review & editing.

Declaration of competing interest

The authors declare that they have no known competing financial interests or personal relationships that could have appeared to influence the work reported in this paper.

Acknowledgments

This work has been supported by Grants: BFU2014-53641-P and BFU2017-85723-P of the Spanish Plan Nacional de I + D + i, and GR21174 and IDA1-19-0055-3 of the Junta de Extremadura. All these Grants have been co-financed by the European Funds for Structural Development (FEDER). Joana Poejo has been funded, in part, by Cafés Delta Foundation (Campo Maior, Portugal). Jairo Salazar has been supported by a predoctoral Fellowship of the Fundación Carolina (Spain). We thank our laboratory technician Ms. Laura Ortega Bermejo for her invaluable technical support with animal handlings and samples preparation for immunohistochemistry.

Appendix A. Supplementary data

Supplementary data to this article can be found online at https://doi.org/10.1016/j.fct.2022.113017.

References

Babaei, P., Eyvani, K., Kouhestani, S., 2021. Sex-independent cognition improvement in response to kaempferol in the model of sporadic Alzheimer's disease. Neurochem. Res. 46, 1480–1486. https://doi.org/10.1007/s11064-021-03289-y.

Bennett, M.L., Bennett, F.C., Liddelow, S.A., Ajami, B., Zamanian, J.L., Fernhoff, N.B., Mulinyawe, S.B., Bohlen, C.J., Adil, A., Tucker, A., Weissman, I.L., Chang, E.F., Li, G., Grant, G.A., Hayden-Gephart, M.G., Barres, B.A., 2016. New tools for studying microglia in the mouse and human CNS. Proc. Natl. Acad. Sci. U.S.A. 113, E1738–E1746. https://doi.org/10.1073/pnas.1525528113.

Brouillet, E., Condé, F., Beal, M.F., Hantraye, P., 1999. Replicating Huntington's disease phenotype in experimental animals. Prog. Neurobiol. 59, 427–468. https://doi.org/10.1016/s0301-0082(99)00005-2.

Brouillet, E., Jacquard, C., Bizat, N., Blum, D., 2005. 3-Nitropropionic acid: a mitochondrial toxin to uncover physiopathological mechanisms underlying striatal degeneration in Huntington's disease. J. Neurochem. 95, 1521–1540. https://doi.org/10.1111/j.1471-4159.2005.03515.x.

Browne, S.E., Ferrante, R.J., Beal, M.F., 1999. Oxidative stress in Huntington's disease. Brain Pathol. 9, 147–163. https://doi.org/10.1111/j.1750-3639.1999.tb00216.x.

Chakraborty, J., Singh, R., Dutta, D., Naskar, A., Rajamma, U., Mohanakumar, K.P., 2014. Quercetin improves behavioral deficiencies, restores astrocytes and microglia, and reduces serotonin metabolism in 3-nitropropionic acid-induced rat model of Huntington's disease. CNS Neurosci. Ther. 20, 10–19. https://doi.org/10.1111/cns.12189.

Cheng, G., Wessels, A., Gourdie, R.G., Thompson, R.P., 2002. Spatiotemporal and tissue specific distribution of apoptosis in the developing chick heart. Dev. Dynam. 223, 119–133. https://doi.org/10.1002/dvdy.1244.

Diaz-Castro, B., Gangwani, M.R., Yu, X., Coppola, G., Khakh, B.S., 2019. Astrocyte molecular signatures in Huntington's disease. Sci. Transl. Med. 11, eaaw8546 https://doi.org/10.1126/scitranslmed.aaw8546.

Escartin, C., Galea, E., Lakatos, A., O'Callaghan, J.P., Petzold, G.C., Serrano-Pozo, A., et al., 2021. Reactive astrocyte nomenclature, definitions, and future directions. Nat. Neurosci. 24, 312–325. https://doi.org/10.1038/s41593-020-00783-4.

Farina, C., Aloisi, F., Meinl, E., 2007. Astrocytes are active players in cerebral innate immunity. Trends Immunol. 28, 138–145. https://doi.org/10.1016/j.it.2007.01.005.

Frost, G.R., Li, Y.M., 2017. The role of astrocytes in amyloid production and Alzheimer's disease. Open Biol 7, 170228. https://doi.org/10.1098/rsob.170228.

Fu, Y., 1995. 3-Nitropropionic acid produces indirect excitotoxic damage to rat striatum. Neurotoxicol. Teratol. 17, 333–339. https://doi.org/10.1016/0892-0362(94)00076-.

Gao, W., Wang, W., Peng, Y., Deng, Z., 2019. Antidepressive effects of kaempferol mediated by reduction of oxidative stress, proinflammatory cytokines and up-regulation of AKT/β-catenin cascade. Metab. Brain Dis. 34, 485–494. https://doi.org/10.1007/s11011-019-0389-5.

Gutierrez-Merino, C., Lopez-Sanchez, C., Lagoa, R., Samhan-Arias, A.K., Bueno, C., Garcia-Martinez, V., 2011. Neuroprotective actions of flavonoids. Curr. Med. Chem. 18, 1195–1212. https://doi.org/10.2174/092986711795029735.

Han, X., Zhao, S., Song, H., Xu, T., Fang, Q., Hu, G., Sun, L., 2021. Kaempferol alleviates LD-mitochondrial damage by promoting autophagy: implications in Parkinson's disease. Redox Biol. 41, 101911 https://doi.org/10.1016/j.redox.2021.101911.

Hawkins, B.T., Davis, T.P., 2005. The blood-brain barrier/neurovascular unit in health and disease. Pharmacol. Rev. 57, 173–185. https://doi.org/10.1124/pr.57.2.4.

He, F., Zhang, S., Qian, F., Zhang, C., 1995. Delayed dystonia with striatal CT lucencies induced by a mycotoxin (3-nitropropionic acid). Neurology 45, 2178–2183. https://doi.org/10.1212/WNL.45.12.2178.

Hernandez-Encinas, E., Aguilar-Morante, D., Morales-Garcia, J.A., Gine, E., Sanz-SanCristobal, M., Santos, A., Perez-Castillo, A., 2016. Complement component 3 (C3) expression in the hippocampus after excitotoxic injury: role of C/EBPβ. J. Neuroinflammation 13, 276. https://doi.org/10.1186/s12974-016-0742-0.

Ho, A.K., Sahakian, B.J., Brown, R.G., Barker, R.A., Hodges, J.R., Ané, M.-N., Snowden, J., Thompson, J., Esmonde, T., Gentry, R., Moore, J.W., Bodner, T., 2003. Profile of cognitive progression in early Huntington's disease. Neurology 61, 1702–1706. https://doi.org/10.1212/01.WNL.0000098878.47789.BD.

Huber-Lang, M., Ekdahl, K.N., Wiegner, R., Fromell, K., Nilsson, B., 2018. Auxiliary activation of the complement system and its importance for the pathophysiology of clinical conditions. Semin. Immunopathol. 40, 87–102. https://doi.org/10.1007/s00281-017-0646-9.

Jin, X., Riew, T.-R., Kim, H.L., Choi, J.-H., Lee, M.-Y., 2018. Morphological characterization of NG2 glia and their association with neuroglial cells in the 3-nitropropionic acid–lesioned striatum of rat. Sci. Rep. 8, 5942. https://doi.org/10.1038/s41598-018-24385-0.

Kaltschmidt, C., Kaltschmidt, B., Neumann, H., Wekerle, H., Baeuerle, P.A., 1994. Constitutive NF-kappa B activity in neurons. Mol. Cell Biol. 14, 3981–3992. https://doi.org/10.1128/mcb.14.6.3981-3992.1994.

Kaltschmidt, C., Kaltschmidt, B., Henkel, T., Stockinger, H., Baeuerle, P.A., 1995. Selective recognition of the activated form of transcription factor NF-kappa B by a monoclonal antibody. Biol. Chem. Hoppe Seyler 376, 9–16. https://doi.org/10.1515/bchm3.1995.376.1.9.

Kulkarni, A.P., Kellaway, L.A., Kotwal, G.J., 2005. Herbal complement inhibitors in the treatment of neuroinflammation. Future strategy for neuroprotection. Ann. N. Y. Acad. Sci. 1056, 413–429. https://doi.org/10.1196/annals.1352.020.

Lagoa, R., Lopez-Sanchez, C., Samhan-Arias, A.K., Gañan, C.M., Garcia-Martinez, V., Gutierrez-Merino, C., 2009. Kaempferol protects against rat striatal degeneration induced by 3-nitropropionic acid. J. Neurochem. 111, 473–487. https://doi.org/10.1111/j.1471-4159.2009.06331.x.

Lahiani-Cohen, I., Touloumi, O., Lagoudaki, R., Grigoriadis, N., Rosenmann, H., 2020. Exposure to 3-nitropropionic acid mitochondrial toxin induces tau pathology in tangle-mouse model and in wild type-mice. Front. Cell Dev. Biol. 7, 321. https://doi.org/10.3389/fcell.2019.00321.

Lee, K.M., MacLean, A.G., 2015. New advances on glial activation in health and disease. World J. Virol. 4, 42–55. https://doi.org/10.5501/wjv.v4.i2.42.

Li, K., Fazekasova, H., Wang, N., Sagoo, P., Peng, Q., Khamr, W., Gomes, C., Sacks, S.H., Lombardi, G., Zhou, W., 2011. Expression of complement proteins, receptors and regulators by human dendritic cells. Mol. Immunol. 48, 1121–1127. https://doi.org/10.1016/j.molimm.2011.02.003.

Li, Y., Severance, E.G., Viscidi, R.P., Yolken, R.H., Xiao, J., 2019. Persistent Toxoplasma infection of the brain induced neurodegeneration associated with activation of complement and microglia. Infect. Immun. 87 https://doi.org/10.1128/IAI.00139-19 e00139-19.

Liddelow, S.A., Guttenplan, K.A., Clarke, L.E., Bennett, F.C., Bohlen, C.J., Schirmer, L., Bennett, M.L., Münch, A.E., Chung, W.-S., Peterson, T.C., Wilton, D.K., Frouin, A., Napier, B.A., Panicker, N., Kumar, M., Buckwalter, M.S., Rowitch, D.H., Dawson, V. L., Dawson, T.M., Stevens, B., Barres, B.A., 2017. Neurotoxic reactive astrocytes are induced by activated microglia. Nature 541, 481–487. https://doi.org/10.1038/nature21029.

Liu, B., Gao, H.-M., Wang, J.-Y., Jeohn, G.-H., Cooper, C.I., Hong, J.-S., 2002. Role of nitric oxide in inflammation-mediated neurodegeneration. Ann. N. Y. Acad. Sci. 962, 318–331. https://doi.org/10.1111/j.1749-6632.2002.tb04077.x.

Lopez-Sanchez, C., Martin-Romero, F.J., Sun, F., Luis, L., Samhan-Arias, A.K., Garcia-Martinez, V., Gutierrez-Merino, C., 2007. Blood micromolar concentrations of kaempferol afford protection against ischemia/reperfusion induced damage in rat brain. Brain Res. 1182, 123–137. https://doi.org/10.1016/j.brainres.2007.08.087.

Lopez-Sanchez, C., Garcia-Martinez, V., Poejo, J., Garcia-Lopez, V., Salazar, J., Gutierrez-Merino, C., 2020. Early reactive A1 astrocytes induction by the neurotoxin 3-nitropropionic acid in rat brain. Int. J. Mol. Sci. 21, 3609. https://doi.org/10.3390/ijms21103609.

Ludolph, A.C., He, F., Spencer, P.S., Hammerstad, J., Sabri, M., 1991. 3-Nitropropionic acid – exogenous animal neurotoxin and possible human striatal toxin. Can. J. Neurol. Sci. 18, 492–498. https://doi.org/10.1017/S0317167100032212.

Maleki, S.J., Crespo, J.F., Cabanillas, B., 2009. Anti-inflammatory effects of flavonoids. Food Chem. 299, 125124 https://doi.org/10.1016/j.foodchem.2019.125124.

Menze, E., Esmat, A., Tadros, M.G., Abdel-Naim, A.B., Khalifa, A.E., 2015. Genistein improves 3-NPA-induced memory impairment in ovariectomized rats: impact of its antioxidant, anti-inflammatory and acetylcholinesterase modulatory properties. PLoS One 10, e0117223. https://doi.org/10.1371/journal.pone.0117223.

Morita, H., Suzuki, K., Mori, N., Yasuhara, O., 2006. Occurrence of complement protein C3 in dying pyramidal neurons in rat hippocampus after systemic administration of kainic acid. Neurosci. Lett. 409, 35–40. https://doi.org/10.1016/j.neulet.2006.09.037.

Nadler, Y., Alexandrovich, A., Grigoriadis, N., Hartmann, T., Rao, K.S.J., Shohami, E., Stein, R., 2008. Increased expression of the gamma-secretase components presenilin-1 and nicastrin in activated astrocytes and microglia following traumatic brain injury. Glia 56, 552–567. https://doi.org/10.1002/glia.20638.

Nakanishi, H., 2020. Microglial cathepsin B as a key driver of inflammatory brain diseases and brain aging. Neural Regen. Res. 15, 25–29. https://doi.org/10.4103/1673-5374.264444.

Nasr, P., Gursahani, H.I., Pang, Z., Bondada, V., Lee, J., Hadley, R.W., Geddes, J.W., 2003. Influence of cytosolic and mitochondrial Ca^{2+}, ATP, mitochondrial membrane potential, and calpain activity on the mechanism of neuron death induced by 3-nitropropionic acid. Neurochem. Int. 43, 89–99. https://doi.org/10.1016/S0197-0186(02)00229-2.

Niccolini, F., Politis, M., 2014. Neuroimaging in Huntington's disease. World J. Radiol. 6, 301–312. https://doi.org/10.4329/wjr.v6.i6.301.

Nishino, H., Kumazaki, M., Fukuda, A., Fujimoto, I., Shimano, Y., Hida, H., Sakurai, T., Deshpande, S.B., Shimizu, H., Morikawa, S., Inubushi, T., 1997. Acute 3-nitropropionic acid intoxication induces striatal astrocytic cell death and dysfunction of the blood-brain barrier: involvement of dopamine toxicity. Neurosci. Res. 27, 343–355. https://doi.org/10.1016/S0168-0102(97)01170-X.

Ouary, S., Bizat, N., Altairac, S., Ménétrat, H., Mittoux, V., Condé, F., Hantraye, P., Brouillet, E., 2000. Major strain differences in response to chronic systemic administration of the mitochondrial toxin 3-nitropropionic acid in rats: implications for neuroprotection studies. Neuroscience 97, 521–530. https://doi.org/10.1016/s0306-4522(00)00020-8.

Park, S.H., Oh, S.R., Jung, K.Y., Lee, I.S., Ahn, K.S., Kim, J.H., Kim, Y.S., Lee, J.J., Lee, H. K., 1999. Acylated flavonol glycosides with anti-complement activity from *Persicaria lapathifolia*. Chem. Pharm. Bull. 47, 1484–1486. https://doi.org/10.1248/cpb.47.1484.

Phillips, W., Shannon, K.M., Barker, R.A., 2008. The current clinical management of Huntington's disease. Mov. Disord. 23, 1491–1504. https://doi.org/10.1002/mds.21971.

Praticò, D., Delanty, N., 2000. Oxidative injury in diseases of the central nervous system: focus on Alzheimer's disease. Am. J. Med. 109, 577–585. https://doi.org/10.1016/S0002-9343(00)00547-7.

Ren, J., Lu, Y., Qian, Y., Chen, B., Wu, T., Ji, G., 2019. Recent progress regarding kaempferol for the treatment of various diseases. Exp. Ther. Med. 18, 2759–2776. https://doi.org/10.3892/etm.2019.7886.

Represa, A., Deloulme, J.C., Sensenbrenner, M., Ben-Ari, Y., Baudier, J., 1990. Neurogranin: immunocytochemical localization of a brain-specific protein kinase C substrate. J. Neurosci. 12, 3782–3792. https://doi.org/10.1523/JNEUROSCI.10-12-03782.

Rosenberg, G.A., 2009. Matrix metalloproteinases and their multiple roles in neurodegenerative diseases. Lancet Neurol. 8, 205–216. https://doi.org/10.1016/S1474-4422(09)70016-X.

Rosenstock, T.R., Carvalho, A.C.P., Jurkiewicz, A., Frussa-Filho, R., Smaili, S.S., 2004. Mitochondrial calcium, oxidative stress and apoptosis in a neurodegenerative disease model induced by 3-nitropropionic acid. J. Neurochem. 88, 1220–1228. https://doi.org/10.1046/j.1471-4159.2003.02250.x.

Ryu, J.K., Nagai, A., Kim, J., Lee, M.C., McLarnon, J.G., Kim, S.U., 2003. Microglial activation and cell death induced by the mitochondrial toxin 3-nitropropionic acid: *In vitro* and *in vivo* studies. Neurobiol. Dis. 12, 121–132. https://doi.org/10.1016/S0969-9961(03)00002-0.

Saleem, S., Zhuang, H., Biswal, S., Christen, Y., Doré, S., 2008. *Ginkgo biloba* extract neuroprotective action is dependent on heme oxygenase 1 in ischemic reperfusion brain injury. Stroke 39, 3389–3396. https://doi.org/10.1161/STROKEAHA.108.523480.

Silva Dos Santos, J., Gonçalves Cirino, J.P., de Oliveira Carvalho, P., Ortega, M.M., 2021. The pharmacological action of kaempferol in central nervous system diseases: a review. Front. Pharmacol. 11, 565700 https://doi.org/10.3389/fphar.2020.565700.

Stanek, L.M., Bu, J., Shihabuddin, L.S., 2019. Astrocyte transduction is required for rescue of behavioral phenotypes in the YAC128 mouse model with AAV-RNAi mediated HTT lowering therapeutics. Neurobiol. Dis. 129, 29–37. https://doi.org/10.1016/j.nbd.2019.04.015.

Stewart, V.C., Sharpe, M.A., Clark, J.B., Heales, S.J.R., 2002. Astrocyte-derived nitric oxide causes both reversible and irreversible damage to the neuronal mitochondrial respiratory chain. J. Neurochem. 75, 694–700. https://doi.org/10.1046/j.1471-4159.2000.0750694.x.

Sun, F., López-Sánchez, C., Martin-Romero, F.J., Luis, L., Gutierrez-Merino, C., Garcia-Martinez, V., 2005. Transfemoral selective "intraluminal wiring" technique for transient middle cerebral artery occlusion in rats. J. Neurosci. Methods 149, 82–89. https://doi.org/10.1016/j.jneumeth.2005.05.008.

Thomas, A., Gasque, P., Vaudry, D., Gonzalez, B., Fontaine, M., 2000. Expression of a complete and functional complement system by human neuronal cells in vitro. Int. Immunol. 12, 1015–1023. https://doi.org/10.1093/intimm/12.7.1015.

Tsang, T.M., Haselden, J.N., Holmes, E., 2009. Metabolomic characterization of the 3-nitropropionic acid rat model of Huntington's disease. Neurochem. Res. 34, 1261–1271. https://doi.org/10.1007/s11064-008-9904-5.

Wang, T., Sun, Q., Yang, J., Wang, G., Zhao, F., Chen, Y., Jin, Y., 2021. Reactive astrocytes induced by 2-chloroethanol modulate microglia polarization through IL-1β, TNF-α, and iNOS upregulation. Food Chem. Toxicol. 157, 112550 https://doi.org/10.1016/j.fct.2021.112550.

Ward, C.P., Redd, K., Williams, B.M., Caler, J.R., Luo, Y., McCoy, J.G., 2002. *Ginkgo biloba* extract: cognitive enhancer or antistress buffer. Pharmacol. Biochem. Behav. 72, 913–922. https://doi.org/10.1016/S0091-3057(02)00768-2.

Zhang, Y., Chen, K., Sloan, S.A., Bennett, M.L., Scholze, A.R., O'Keeffe, S., Phatnani, H.P., Guarnieri, P., Caneda, C., Ruderisch, N., Deng, S., Liddelow, S.A., Zhang, C., Daneman, R., Maniatis, T., Barres, B.A., Wu, J.Q., 2014. An RNA-sequencing transcriptome and splicing database of glia, neurons, and vascular cells of the cerebral cortex. J. Neurosci. 34, 11929–11947. https://doi.org/10.1523/JNEUROSCI.1860-14.2014.

Zhao, J., O'Connor, T., Vassar, R., 2011. The contribution of activated astrocytes to Aβ production: implications for Alzheimer's disease pathogenesis. J. Neuroinflammation 8, 150. https://doi.org/10.1186/1742-2094-8-150.